NASA Technical Memorandum 89868

Analysis of an Advanced Technology Subsonic Turbofan Incorporating Revolutionary Materials

Gerald Knip, Jr.
Lewis Research Center
Cleveland, Ohio

May 1987

NASA

ANALYSIS OF AN ADVANCED TECHNOLOGY SUBSONIC TURBOFAN INCORPORATING REVOLUTIONARY MATERIALS

Gerald Knip, Jr.
National Aeronautics and Space Administration
Lewis Research Center
Cleveland, Ohio 44135

E-3542

SUMMARY

Successful implementation of revolutionary composite materials in an advanced turbofan offers the possibility of further improvements in engine performance and thrust-to-weight ratio relative to current metallic materials. The present analysis determines the approximate engine cycle and configuration for an early 21st century subsonic turbofan incorporating all composite materials. The advanced engine is evaluated relative to a current technology baseline engine in terms of its potential fuel savings for an intercontinental quadjet having a design range of 5500 nmi and a payload of 500 passengers.

The resultant near optimum, uncooled, two-spool, advanced engine has an overall pressure ratio of 87, a bypass ratio of 18, a geared fan, and a turbine rotor-inlet temperature of 3085 °R. Relative to the baseline, the advanced engine yields a 22 percent improvement in cruise TSFC and a 36-percent reduction in engine weight. Together these improvements result in a 33-percent fuel saving for the specified mission.

Various advanced composite materials are used throughout the engine. For example, advanced polymer composite materials are used for the fan and the low pressure compressor (LPC). A Ti metal matrix composite is used for the high pressure compressor (HPC) to accommodate the higher operating temperatures. Ceramic composites are used for the combustor and both turbines.

The advanced engine's performance includes aggressive component efficiencies based on these new materials and structural changes such as swept fan and compressor blades, uncooled turbines, reduced hub-tip ratios, higher blade loadings, reduced clearances, and three-dimensional design concepts.

INTRODUCTION

Over the past 40 yr, advanced turbine engines have been the pacing item in terms of the U.S. competitive edge in commercial aviation. During this period the specific fuel consumption (TSFC) of subsonic turbine engines has been reduced by about 40 percent. This reduction has been achieved through improvements in component aerodynamics, materials, and turbine cooling effectiveness. Improvements in materials and turbine cooling have resulted in the maximum turbine temperature being increased from 1000 to 2600 °F. Engine overall pressure ratios have increased from 5 to over 38 (refs. 1 to 3), and bypass ratios from 0 (turbojet) to 7 (turbofan). Advanced metallic materials have also allowed tip speeds and blade loading to be increased resulting in fewer but more efficient stages and lighter weight components. Composite materials are just beginning to be used in turbine engines and then only for nonrotating components.

Successful implementation of revolutionary composite materials (e.g., polymer, metal matrix, and high-temperature nonmetallic composites) in an advanced turbofan offers the possibility of still further improvements in engine performance and thrust-to-weight ratios relative to current conventional materials (i.e., titanium, steel, and superalloys). Advanced composite materials with advanced structures will allow higher tip speeds and thinner blades resulting in fewer and more efficient stages. Advanced nonmetallic composites will allow turbines to operate uncooled at higher turbine inlet temperatures resulting in higher overall pressure ratios and bypass ratios, thereby improving performance. Lower material densities and, therefore, reduced blade weights will result in lower stresses and reduced engine weight. Advanced structures such as drum construction rather than disks will also result in lower engine weights.

The purpose of this study was to (1) determine the approximate cycle and configuration for a turbofan engine incorporating revolutionary all-composite materials, and (2) evaluate the potential fuel saving relative to an engine using current technology (current material) for a commercial subsonic transport mission. This was done by conducting both engine cycle and flowpath studies.

ANALYSIS

Mission

For this study, an intercontinental quadjet having a design range of 5500 nmi and a payload of 500 passengers was assumed. Engines having a thrust of about 10 000 lb at Mach 0.8 and 35 000 ft would be required. This size engine was, therefore, considered in the present study. Sensitivity factors for engine performance (TSFC) and weight were used to determine changes in fuel consumption.

Baseline Engine

The baseline engine used for the study is similar to the Maximum Efficiency Energy Efficient Engine of reference 4. It is a two-spool engine with the fan and the low pressure compressor directly driven by the low pressure turbine. The engine is based on current technology. Compressor pressure ratios are listed in table I along with the turbine rotor-inlet temperature. Air for cooling the turbine is extracted at the exit of the high pressure compressor. Turbine cooling requirements for the baseline engine are based on the method outlined in reference 5. Compressor exit bleed requirements for turbine cooling are based on values for cooling effectiveness assuming advanced convection cooling with trailing edge ejection. Current allowable bulk metal temperatures were used for the vanes (2200 °R) and blades (2100 °R). Based on the turbine stage cooling requirements, the stage efficiency was corrected accordingly.

Advanced Engines

Cycle study. - For the advanced engine, a cycle study was conducted to define an engine cycle based on thrust specific fuel consumption (TSFC) as the figure of merit. TSFC is influenced by engine cycle parameters such as overall pressure ratio (OPR), bypass ratio (BPR), turbine rotor-inlet temperature (T_{41}), component efficiencies, and component configurations. An in-house design-point study program (FACE) was used to determine design point TSFC's and to screen various separate flow turbofan configurations. Inputs for this program include fan and compressor pressure ratios, number of stages, type of compressor (axial or centrifugal), turbine rotor-inlet temperature, number of spools, number of turbine stages, and type of turbine cooling configuration.

For the present study, two levels of compressor and turbine efficiencies were considered. One level represents current technology as opposed to the aggressive second level, which represents advanced technology. Based on discussions with NASA component personnel and a study conducted under NASA contract (ref. 4), higher component efficiencies due to the use of advanced composite materials were postulated based on components having thinner blades, higher tip velocities, uncooled turbines, improved clearance control, and reduced hub-tip ratios in addition to making more efficient use of advanced three-dimensional, CFM design technology. Efficiencies for the compressors and turbines are determined on the basis of stage pressure ratio and work factor ($gJ\ \Delta H/N/U_m^2$), respectively. Symbols are defined in appendix A. Compressor and turbine efficiencies are then corrected for size effects. Turbine efficiencies are also corrected to account for clearance and turbine cooling effects.

Advanced Components and Materials

Advanced materials currently being considered to allow future turbine engines to operate efficiently at high temperatures and pressures are shown in figure 1.

Compressors. - Both polymer and metal matrix composites (refs. 6 to 9) are candidates for fan blades and the front stages of a compressor. For the latter stages operating at higher temperatures metal matrix and intermetallics are possibilities. The rotor may consist of a drum for retaining the blades (outside the scope of the present study).

Combustor. - Advanced materials are also being considered for future turbine engine combustors. These materials included oxide dispersion strengthened (ODS) superalloys and nonmetallic composites, such as ceramic composites and carbon-carbon. These materials would enable the combustor to be operated at higher temperatures with little or no cooling.

Turbines. - The development of improved materials and better methods of cooling to attain higher turbine temperatures has been one of the primary methods for achieving more efficient and higher thrust-to-weight ratio engines. The potential use temperatures for various materials for both vanes and blades are shown in figures 2 and 3. For both vanes and blades, nonmetallic composites such as ceramic composites and carbon-carbon C-C (refs. 10 to 12) may permit use temperatures as high as 3460 and 4460 °R, respectively. With allowable use temperatures of this magnitude, there would be no need for turbine cooling.

Nozzles. - Advanced materials such as nonmetallic composites are also being considered for turbine engine nozzles.

Flowpath. - Based on the cycle studies, flowpaths for selected engines were then determined using NNEP (ref. 13) and the NASA weight code (ref. 14). Thermodynamic inputs required for the weight code are determined in NNEP. The weight program determines the weight of each component in the engine such as compressors, burner, turbines, frames, gearbox, and accessories. Component weights are determined on the basis of a preliminary design approach considering stress levels, maximum temperature, material density, geometry, stage loading, and hub-tip ratio. Based on the advanced materials of figure 1 selected for each component and the data presented in reference 4, the weight program input parameters for the baseline engine were updated to account for differences between the baseline turbofan and the advanced turbofan using advanced composite materials. The material for each component was selected on the basis of maximum component temperature. Relative to a current aluminum or magnesium gearbox housing, a metal matrix composite may result in a stiffer housing. However, for this study no weight advantage was considered.

Installed performance. - The uninstalled performances for the baseline and the advanced engines were corrected for nacelle drag. Based on the differences in installed TSFC and weight between the two engines, fuel savings were determined using mission sensitivity factors (ref. 15). These sensitivity factors were determined from a mission analysis of an intercontinental, turbofan powered transport having a range of 5500 nmi and a payload of 500 passengers.

RESULTS AND DISCUSSION

To minimize TSFC for an advanced turbofan engine providing a thrust of 10 000 lb at Mach 0.8 and 35 000 ft, the following parameters were considered: turbine rotor-inlet temperature (T_{41}), fan and compressor pressure ratios, overall pressure ratio (OPR), bypass ratio (BPR), and number of stages for a two-spool engine.

Effect of Advanced Engine Design Parameters on Performance

Turbine rotor-inlet temperature (T_{41}). - The level of turbine inlet temperature can affect not only engine performance (TSFC), but also engine size and, therefore weight. The effect of T_{41} on TSFC for a range of OPR's is shown in figure 4. For these advanced engines, the turbines are uncooled. The pressure ratio for the fan (1.55(bypass)/1.4(core)) and the low pressure compressor (LPC) were held constant while the pressure ratio of the high pressure compressor (HPC) was varied to achieve the specified OPR. The number of axial stages for the LPC and the HPC were fixed at 3 and 11, respectively. Although fewer stages for the HPC could be used for the lower pressure ratios, this would result in lower compressor efficiencies and, therefore, a higher TSFC. Two axial stage turbines were used for the high pressure turbine (HPT) and five for the low pressure turbine (LPT). Bypass ratio was optimized for each cycle with respect to TSFC. Turbine inlet temperatures (T_{41}) between 2760 and 3085 °R have a small effect on TSFC (fig. 4) due in part to the aggressive component efficiencies for the advanced engine. However, increasing the OPR from 40 (current technology) to 100 results in about an 8.5 percent decrease in TSFC. The effect of turbine temperature on specific thrust (based

on core flow) is shown in figure 5. Increasing T_{41} from 2760 to 3085 °R results in a 35 percent increase in specific thrust. A higher T_{41} results in a somewhat higher specific thrust but also a higher TSFC. Since fuel consumption is more sensitive to TSFC than engine size, and therefore weight, a temperature of 3085 °R was selected.

Fan pressure ratio. - The effect of fan pressure ratio (and therefore BPR) on TSFC is shown in figure 6. Again, the LPC pressure ratio was fixed at 2 and the HPC pressure ratio varied. Decreasing the fan pressure ratio from 1.78 to 1.33 results in about a 7 percent decrease in TSFC. Lower fan pressure ratios with their associated lower tip speeds can be accommodated by means of a gearbox without penalizing turbine efficiency or turbine weight. For an OPR of 100, figure 7 shows the effect of BPR on TSFC. The optimum BPR increases from 18 to 28 as fan pressure ratio is decreased from 1.55 to 1.33. Correspondingly, TSFC decreases by 2.5 percent. However, since the higher BPR would result in a significant increase in engine size and, therefore drag, a fan pressure ratio of 1.55 was selected for the advanced engine.

Low pressure compressor. - Whereas the fan is connected to the low pressure turbine by means of a gearbox, the LPC is directly connected to the turbine. Operating the LPC at the same speed as the turbine increases the tip speed, resulting in fewer stages for the same pressure ratio. Increasing the pressure ratio of the three-stage LPC from 2 to 2.8 (fig. 8) has almost no effect on TSFC. Although the pressure ratio of the LPC does not affect performance, it may have to be modified to change the required pressure ratio of the HPC when one considers component diameters for the flowpath. To reduce the pressure ratio of the HPC, an initial pressure ratio of 2.8 for the LPC was selected for the advanced engine. Based on the relatively small penalty associated with reducing the OPR from 100 to 87 (fig. 6), an OPR of 87 was selected for the advanced engine.

High Pressure Compressor (HPC). - Current technology all-axial HPC's have an average stage pressure ratio of about 1.3. Using this as the average stage pressure ratio, the HPC for an OPR of 60 and 87 would require ~11 and 13 stages, respectively. For an OPR of 87, the effect on TSFC of reducing the number of HPC stages from 13 to 10 is minor (fig. 9). However, 10 or 11 stages may be advantageous in terms of engine length, weight, and cost. As a result the average stage pressure ratio would increase to 1.39 and 1.35, respectively. These increased pressure ratios can be achieved by means of higher tip speeds and/or increased blade loading.

Axial-centrifugal HPC. - In addition to the all-axial high pressure compressor previously discussed, an axial-centrifugal HPC was also considered (fig. 10). Figure 10 shows the optimum pressure ratio split in terms of TSFC for various axial-centrifugal compressors having an overall pressure ratio of 87. At these high pressure ratios, it may be necessary to replace some of the latter axial stages (because of minimum blade height limitations of ~1/2 in.) with a centrifugal stage. TSFC decreases as the number of axial stages is increased from 3 to 5 due to the higher efficiency of the axial stages. The optimum pressure ratio for the centrifugal stage decreases from about 6 to 4 as the number of axial stages increases from 4 to 5. The average pressure ratio for the axial stage is ~1.47. Because of the slightly lower TSFC (fig. 9) for the all-axial compressor, it was selected for the advanced engine.

High pressure turbine (HPT). - The actual stage mean velocity of the HPT depends on the RPM of the HPC and/or the turbine work factor ($gJ\ \Delta H/N/U_m^2$).

Currently mean velocities are of the order of 1400 ft/sec. Figure 11 shows the effect on TSFC of increasing the mean velocity from 1500 to 1600 ft/sec for a HPT consisting of 2 to 4 stages. Based on these results the choice as to mean velocity will depend more on the engine flowpath and weight than TSFC.

Low pressure turbine (LPT). - For direct drive fans, the mean velocity of current LPT's is about 900 ft/sec. With a geared fan, such as would be used on the advanced engine, the mean velocity of the LPT could be increased, thereby, reducing the stage work factor and increasing the turbine efficiency. Figure 12 shows the effect on TSFC of increasing the mean velocity and varying the number of stages. The required expansion ratio for the cycle is about 20. Thus five to possibly as many as seven turbine stages may be required. Again the flow path must be considered before selecting the number of LPT stages and/or the mean velocity.

Advanced Engine Preliminary Definition

Based on the initial cycle and configuration studies the two-spool, separate flow, advanced turbofan at the cruise design point is defined as follows:

Fan pressure ratio: 1.55/1.4
Bypass ratio: 18
LPC three-axial stages: P/P = 2.8
HPC eleven-axial stages: P/P = 22.2
Turbine rotor-inlet temperature: T_{41} = 3085 °R
HPT: three-axial stages
LPT: five-axial stages
Bleed: 0.0

The number of stages for the various components was considered again in the flowpath portion of the study.

Advanced Engine Flowpath

Cycle and geometrical tradeoffs. - To this point, cycle studies have identified the pressure ratios, turbine temperature, bypass ratio, and the configuration resulting in about the minimum TSFC for the advanced engine. However, to optimize the engine in terms of TSFC and weight, the engine flowpath must be considered to identify possible tradeoffs required of the cycle to achieve an acceptable gas path geometry. For example, to reduce the number of stages of compression, blade loading, tip speed, and stress levels must be considered along with pressure ratio and efficiency. The compressor in turn affects the dimensions of the turbine based on the loading parameter resulting from the cycle study. A short study of the flowpath involving various cycle and geometrical tradeoffs was, therefore, undertaken. These tradeoffs are discussed in detail in appendix B and summarized below.

Comparison of advanced and baseline engines. - Based on the flowpath studies, various component configurations, tip speeds, and loadings resulting from the cycle study were modified. The number of stages for the LPC was decreased from three to two in order to save weight. The number of HPT stages was reduced from three to two while the tip velocity was increased by about 200 ft/sec. As a result the loading parameter decreased from 2.0 to 1.54.

In addition the loading parameter for the LPT was increased from 1.52 to 1.86. These changes reduced the length of the transition duct between the HPT and the LPT in addition to reducing engine weight. The resulting flowpath for the advanced turbofan engine is shown in figure 13. For purposes of comparison, the flowpath for the baseline engine is shown in figure 14. The fan diameter is smaller for the baseline because of its lower bypass ratio. Core radii for the advanced engine are, in general, smaller due to the higher tip velocities. Engines having higher bypass ratios and a direct drive fan usually have a longer transition section between the turbines so as to achieve higher efficiencies for the required work loads. This can be seen by comparing figures 13 and 14.

Parameters resulting from the cycle and the flowpath studies for the advanced engine are compared in tables II and III with those for the baseline engine. Table II compares various geometric parameters, the number of stages, and the number of rotor blades. Table III compares the cycles, and flowpath temperatures and pressures. Engine OPR and turbine rotor-inlet temperature (T_{41}) increased from 42.5 and 2775 °R for the baseline engine to 87 and 3085 °R for the advanced turbofan. Although the advanced engine operates at a higher T_{41}, it is uncooled due to the higher use temperature of the advanced materials. The higher OPR is achieved in one less stage of compression. Because of the higher operating pressure ratios, temperatures exiting the various components are in general higher.

Based on temperatures associated with the LPT of the advanced engine, a current material (density of 0.3 lb/in.) could be considered for this component. However, an advanced material such as a ceramic composite (density of 0.115 lb/in.^{3}) would reduce the weight of the engine by 7.5 percent, figure 15. Advanced materials considered for the other components of the advanced engine are listed in table IV.

Figure 16 compares the uninstalled performance of the selected advanced turbofan with that of the baseline engine. On an uninstalled basis the advanced engine results in a 23 percent reduction (improvement) in TSFC.

The uninstalled performance for both engines was then corrected for nacelle drag based on the advanced nacelle geometry (ref. 4) specified in table 5. The advanced nacelle is compared with a current turbofan nacelle in figure 17. The pressure drag was considered to be equal to 50 percent of the friction drag. On an installed performance basis, the TSFC of the advanced turbofan engine is 22 percent lower than the baseline.

In terms of weight, the advanced engine is 36 percent lighter than the baseline (fig. 18). This is due to both the lower densities of the advanced materials and the increase in the turbine rotor-inlet temperature. The higher turbine temperature decreases the size of the engine for a given thrust and, therefore, its weight. The advanced engine with its improved TSFC and reduced weight results in a 33.5 percent fuel savings relative to the baseline for an intercontinental quadjet having a range of 5500 nmi and a payload of 500 passengers (fig. 19).

CONCLUSIONS

The selected cycle resulting from using advanced materials for an advanced technology (2010), subsonic turbofan engine has an overall pressure ratio of 87, a bypass ratio of 18, a gear driven fan, and a turbine rotor-inlet temperature at cruise of 3085 °R. Polymer and metal matrix composites are used in the cool sections of the engine and ceramic composites in the hot sections. As a result the turbines are uncooled.

In addition to the higher turbomachinery component efficiencies postulated from the use of advanced composite materials, these materials are estimated (based on a clean sheet design approach) to result in the following improvements for an advanced engine with a geared fan relative to a current technology baseline engine.

1. A 23 percent improvement in uninstalled engine TSFC at the cruise condition (M.8/35K ft)
2. A 36 percent decrease in engine weight
3. A 33.5 percent fuel savings for an intercontinental transport having a range of 5500 nmi, and a payload of 500 passengers

REFERENCES

1. Gray, D.E.: Study of Turbofan Engines Designed for Low-Energy Consumption. (PWA-5318, Pratt and Whitney Aircraft; NASA Contract NAS3-19132) NASA CR-135002, 1976.

2. Neitzel, R.C.; Hirschkron, R.; and Johnston, R.F.: Study of Turbofan Engines Designed for Low Energy Consumption. (R76AEG432, General Electric Co.; NASA Contract NAS3-19201) NASA CR-135053, 1976.

3. Knip, G.: Preliminary Study of Advanced Turbofans for Low Energy Consumption. NASA TM X-71663, 1975.

4. Gray, D.E.; and Gardner, W.B.: Energy Efficient Engine Program Technology Benefit/Cost Study, Vol. 2, (PWA-5594-251-VOL-2, Pratt and Whitney Aircraft; NASA Contract NAS3-20646) NASA CR-174766-VOL-2, 1983.

5. Gauntner, J.W.: Algorithm for Calculating Turbine Cooling Flow and the Resulting Decrease in Turbine Efficiency. NASA TM-81453, 1980.

6. Blecherman, S.S.; and Stankunas, T.M.: Composite Fan Exit Guide Vanes for High Bypass Ratio Gas Turbine Engines. J. Aircr., vol. 19, no. 12, Dec. 1982, pp. 1032-1037.

7. Stoltza, L.; and Graff, J.: Boron Aluminum Blades and Vanes. AIAA Paper 81-1359, July 1981.

8. Gray, H.R.; Levine, S.R.; and Signorelli, R.A.: Turbine Engine Materials. Tactical Aircraft Research and Technology, Vol. 1, Pt. 2, NASA CP-2162-VOL-1-PT-2, 1981, pp. 471-494.

9. McDanels, D.L.; and Hoffman, C.A.: Microstructure and Orientation Effects on Properties of Discontinuous Silicon Carbide/Aluminum Composites. NASA TP-2302, 1984.

10. Brooks, A.; and Bellin, A.I.: Benefits of Ceramics to Gas Turbines. Ceramics for Turbine Engine Applications, AGARD-CP-276, AGARD, France, 1980.

11. Signorelli, R.A.: High Temperature Composites - Status and Future Directions. Progress in Science and Engineering of Composites, T. Hayashi, K. Kawata, and S. Umekawa, eds., North Holland, 1982, pp. 37-48. (Also, NASA TM-82929.)

12. DiCarlo, J.A.: High Performance Fibers for Structurally Reliable Metal and Ceramic Composites. NASA TM-86878, 1984.

13. Fishbach, L.H.; and Caddy, M.J.: NNEP: The Navy-NASA Engine Program. NASA TM X-71857, 1975.

14. Onat, E.; and Klees, G.W.: A Method to Estimate Weight and Dimensions of Large and Small Gas Turbine Engines. NASA CR-159481, 1979.

15. Gray, D.E.: Energy Efficient Engine Preliminary Design and Integration Study. (PWA-5500-18, Pratt and Whitney Aircraft; NASA Contract NAS3-20628) NASA CR-135396, 1978.

TABLE I. - BASELINE TURBOFAN ENGINE

M 0.8/35 000 ft

Fan pressure ratio	1.65
Bypass ratio	7.2
Low pressure compressor P/P	1.84
High pressure compressor P/P	14.0
Combustor $\Delta P/P$	0.044
Turbine rotor-inlet temperature, °R	2775
Turbine cooling air, percent	12

TABLE II. - COMPARISON OF FLOW PATH PARAMETERS

	Baseline	Advanced
Fan		
Hub/tip ratio	0.34	0.26
Blade solidity	0.94	0.94
First blade AR	4	3
Blade material density	0.168	0.05
Corrected tip velocity, fps	1444	1134
Number of rotor blades	35	23
Number of stages	1	1
LPC		
Hub/tip ratio	0.82	0.77
Blade solidity	1.1	0.63
First blade AR	2.4	2.0
Maximum rotor speed, rpm	3781	11 046
Corrected tip velocity, fps	683	1723
Blade material density	0.168	0.05
Number of rotor blades	400	74
Compressor design type	Const. hub radius	
Number of stages	4	2
HPC		
Hub/tip ratio	0.56	0.49
Blade solidity	0.8	0.8
First blade AR	1.8	1.8
Max rotor speed, rpm	13 798	20 212
Corrected tip velocity, fps	1285	1392
Blade material density	0.3	0.13
Number of rotor blades	827	548
Compressor design type	Const. tip radius	Const. mean radius
Number of stages	10	11
HPT		
Turbine loading parameter $gJ\,\Delta H/N/V_m^2$	1.11	1.54
Blade solidity	0.25	0.25
First blade AR	1.7	2
Blade material density	0.3	0.115
Number of rotor blades	76	84
Turbine design type	Const. mean radius	
Number of stages	2	2
LPT		
Turbine loading parameter	2.38	1.86
Blade solidity	0.44	0.46
First blade AR	3	3
Blade material density	0.3	0.115
Number of rotor blades	404	332
Turbine design type	Const. hub radius	
Number of stages	5	5

TABLE III. - ENGINE COMPARISON

Cycle parameters M 0.8/35K ft

	Fan P/P	Bypass ratio	LPC P/P	HPC P/P	OPR	T_{41}, °R
Baseline	1.65	7.2	1.84	14	42.5	2775
Advanced	1.55	18.1	2.8	22.2	87	3085

Flow path temperatures and pressures

	Inlet	Bypass	LPC exit	HPC exit	HPT inlet	HPT exit	LPT exit
Baseline							
T_T, °R	445	522	633	1402	2775	1901	1264
P_T, psi	5.3	8.7	15.9	223	213	53.6	8.8
Advanced							
T_T, °R	445	507	676	1657	3085	2278	1109
P_T, psi	5.3	8.1	20.6	457	441	108	4.8

TABLE IV. - ADVANCED ENGINE MATERIALS

Component	Material	Density, lb/in^3
Fan	Polymer composite	0.05
LPC	Polymer composite	.05
HPC	Ti metal matrix composite	.13
Combustor	Ceramic composite	.115
HPT	Ceramic composite	.115
LPT	Ceramic composite	.115
Shaft	Ti metal matrix composite	.13

TABLE V. - NACELLE GEOMETRY

Parameter	Baseline	Advanced
Fan cowl $(L/D)_{max}$	1.0	1.0
Fan cowl thickness ratio, D_{max}/D_{tip}, σ	1.2	1.2
Fan hub/fan tip, D_{hub}/D_{tip}	0.38	0.26
Fan specific flow, K, $lb/sec/ft^2$	43	47
Diameter ratio of scrubbed surface	0.7	0.7
Fineness ratio of scrubbed surface	2	2

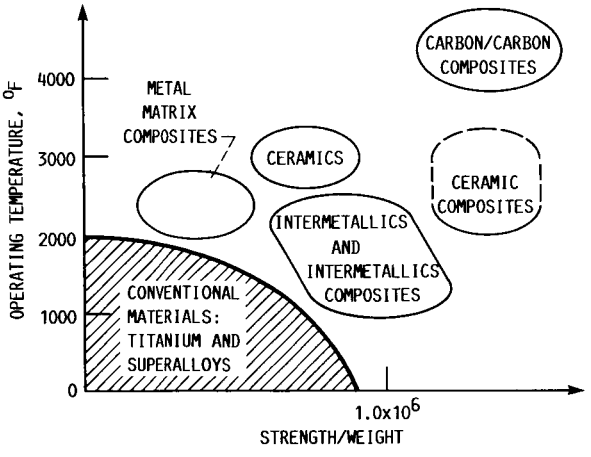

FIGURE 1. - POSSIBLE ADVANCED MATERIALS FOR FUTURE TURBINE ENGINES.

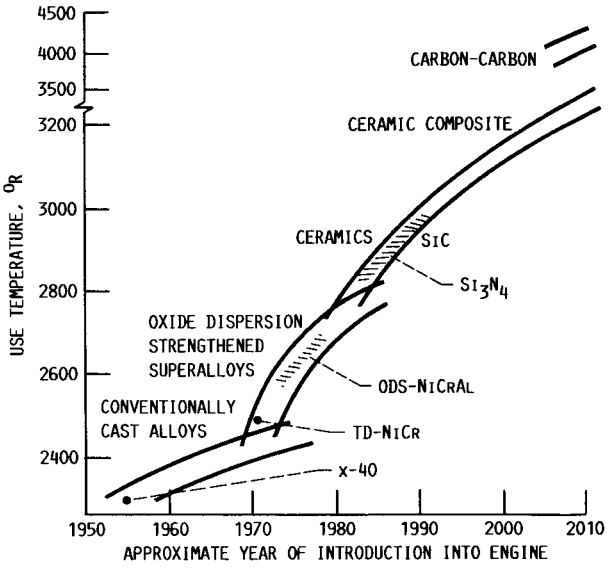

FIGURE 2. - TEMPERATURE TRENDS OF TURBINE VANE MATERIALS.

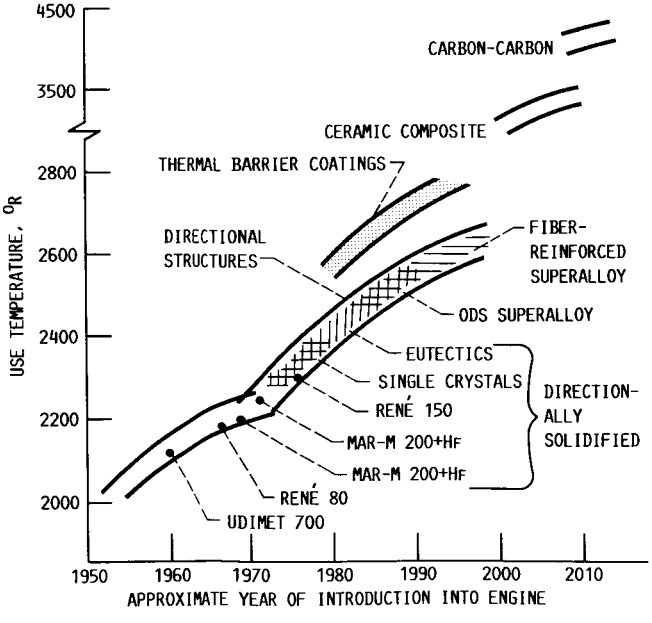

FIGURE 3. - TEMPERATURE TRENDS OF TURBINE BLADE MATERIALS.

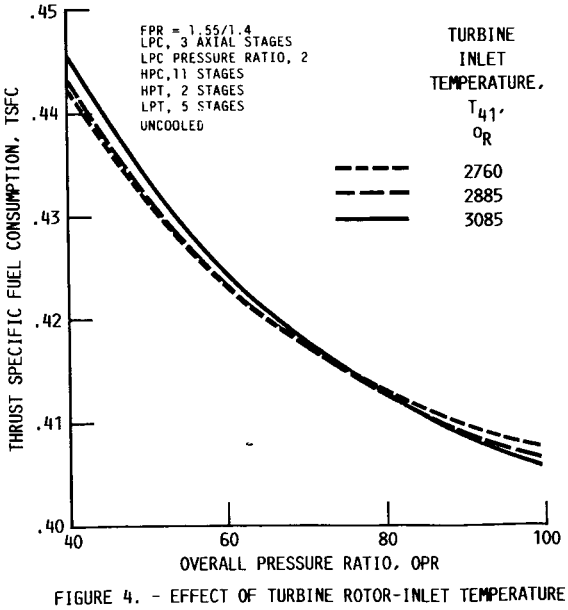

FIGURE 4. - EFFECT OF TURBINE ROTOR-INLET TEMPERATURE ON PERFORMANCE OF ADVANCED TURBOFAN AS FUNCTION OF OVERALL PRESSURE RATIO.

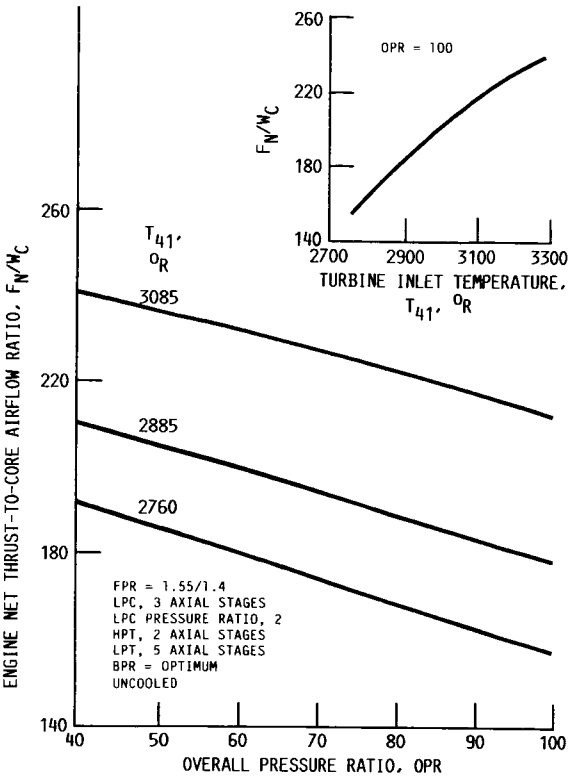

FIGURE 5. - VARIATION IN ENGINE SPECIFIC THRUST WITH TURBINE ROTOR-INLET TEMPERATURE AS FUNCTION OF OVERALL PRESSURE RATIO.

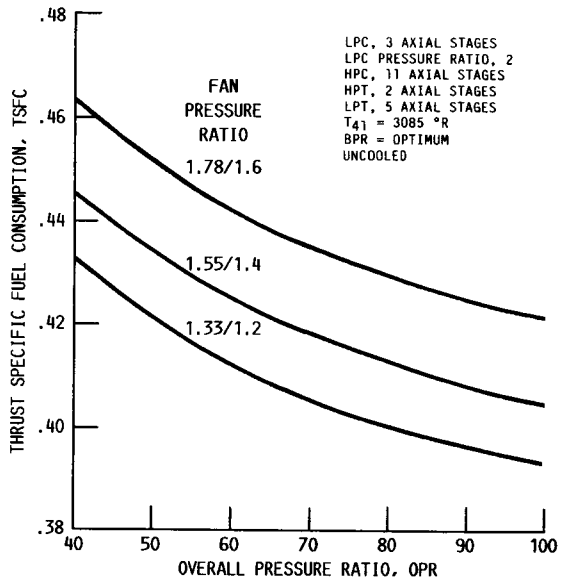

FIGURE 6. - ENGINE PERFORMANCE VERSUS OVERALL PRESSURE RATIO FOR RANGE OF FAN PRESSURE RATIOS.

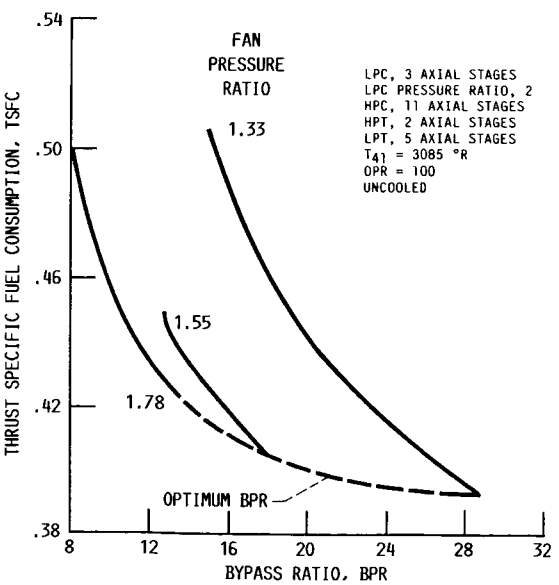

FIGURE 7. - OPTIMUM BYPASS RATIO IN TERMS OF ENGINE PERFORMANCE FOR RANGE OF FAN PRESSURE RATIOS.

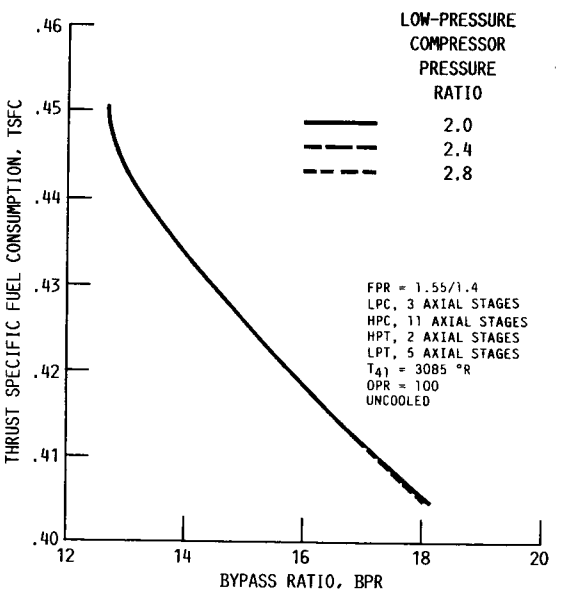

FIGURE 8. - EFFECT OF PRESSURE RATIO FOR THREE-STAGE AXIAL LOW PRESSURE COMPRESSOR ON ENGINE PERFORMANCE.

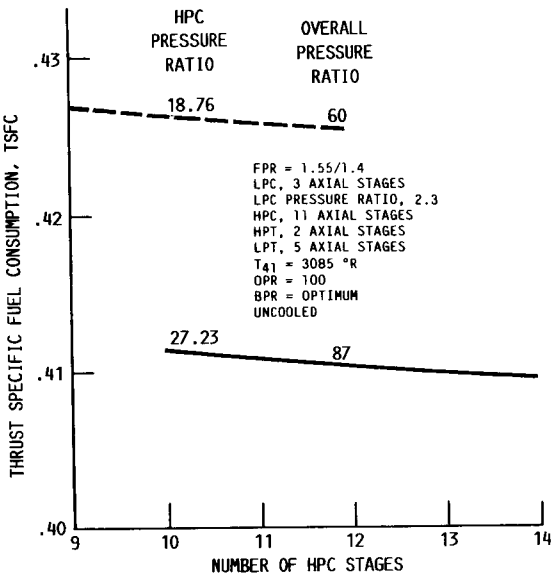

FIGURE 9. - VARIATION IN ENGINE PERFORMANCE AS FUNCTION OF NUMBER OF HIGH-PRESSURE COMPRESSOR STAGES.

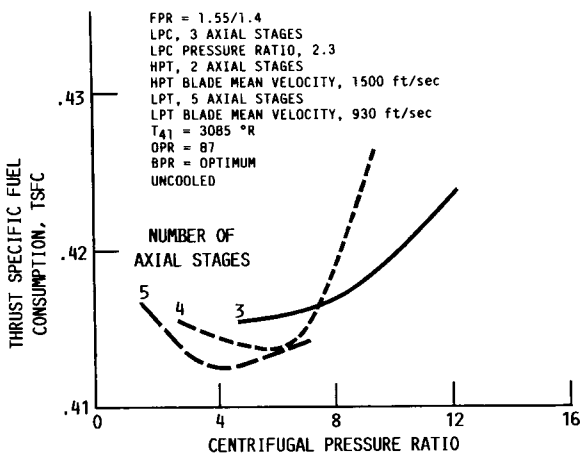

FIGURE 10. - EFFECT OF VARIOUS AXIAL-CENTRIFUGAL HIGH-PRESSURE COMPRESSORS ON PERFORMANCE OF ADVANCED TURBOFAN.

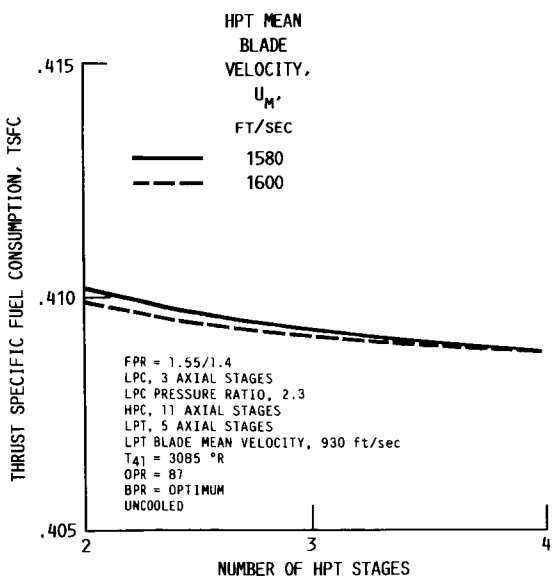

FIGURE 11. - VARIATION IN ENGINE PERFORMANCE AS FUNCTION OF NUMBER OF HIGH-PRESSURE TURBINE STAGES AND MEAN BLADE VELOCITY.

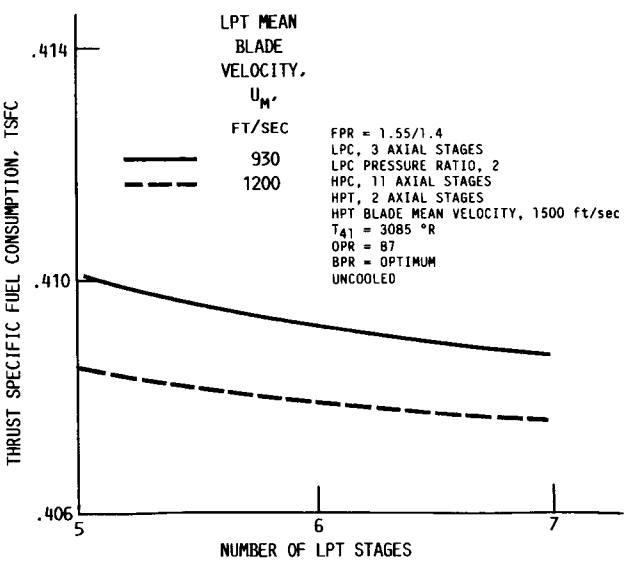

FIGURE 12. - VARIATION IN ENGINE PERFORMANCE AS FUNCTION OF NUMBER OF LOW-PRESSURE TURBINE STAGES AND MEAN BLADE VELOCITY.

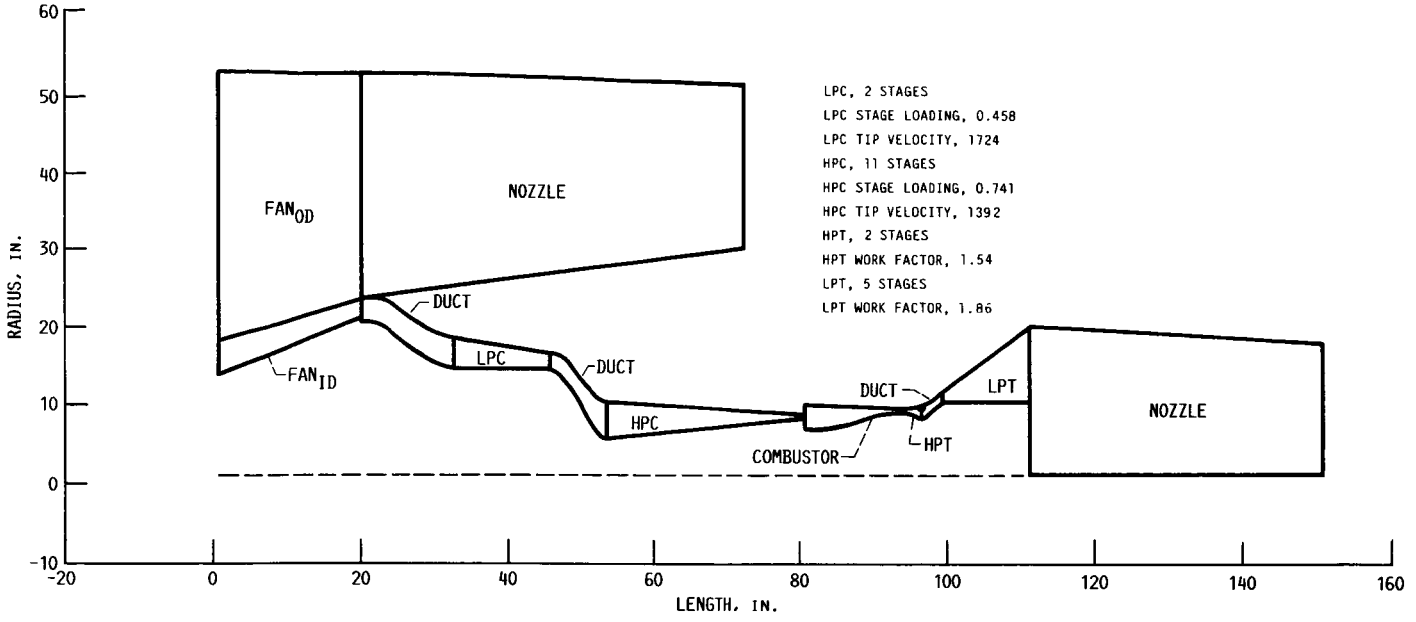

FIGURE 13. - ADVANCED ENGINE FLOWPATH; TOTAL ENGINE WEIGHT, 4866 LB.

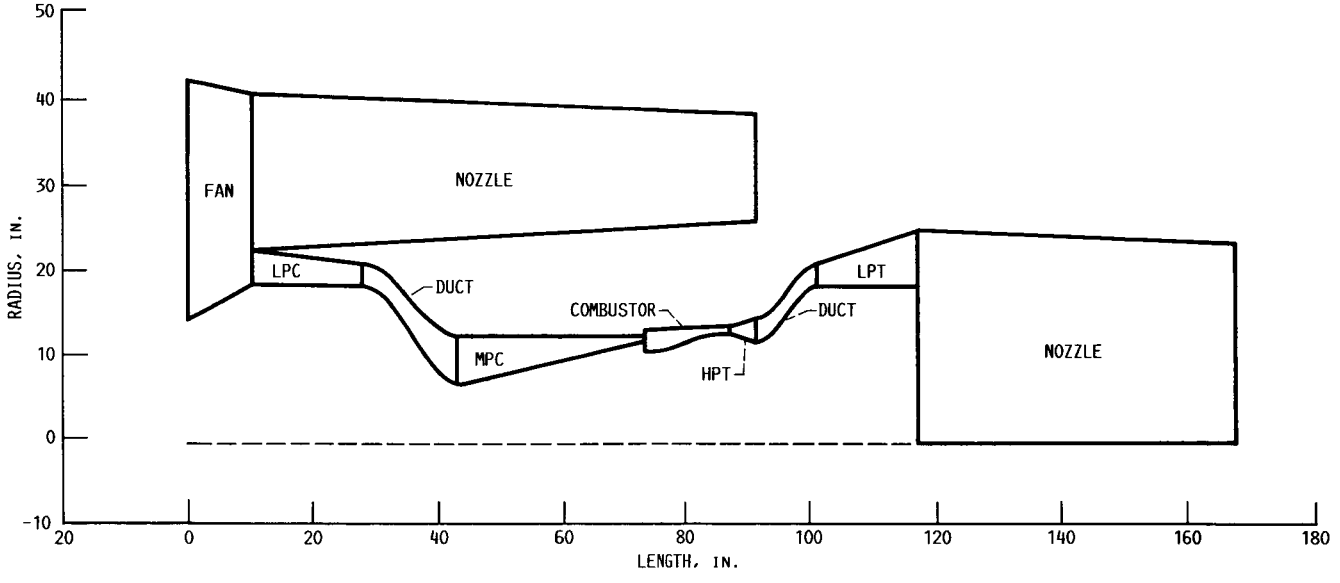

FIGURE 14. - BASELINE ENGINE FLOWPATH; TOTAL ENGINE WEIGHT, 6980 LB.

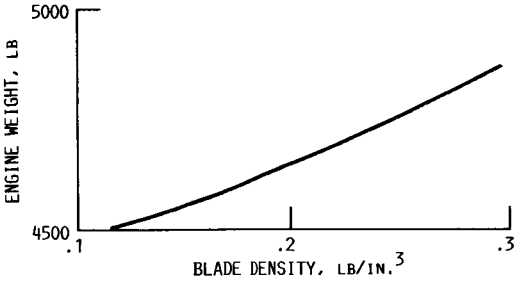

FIGURE 15. - ADVANCED ENGINE WEIGHT VERSUS LOW-PRESSURE TURBINE BLADE DENSITY.

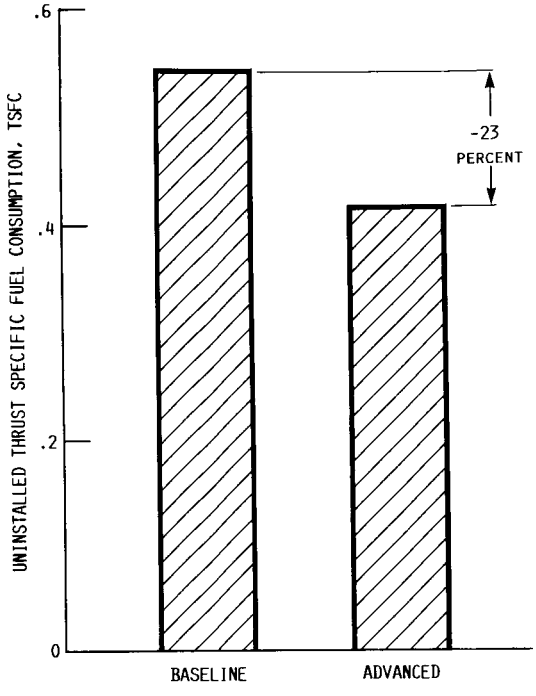

FIGURE 16. - UNINSTALLED TSFC COMPARISON FOR THE BASELINE AND THE ADVANCED TURBOFAN.

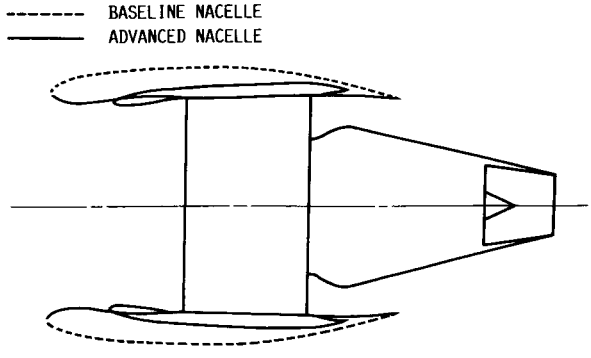

FIGURE 17. - COMPARISON OF ADVANCED AND BASELINE ENGINE NACELLE.

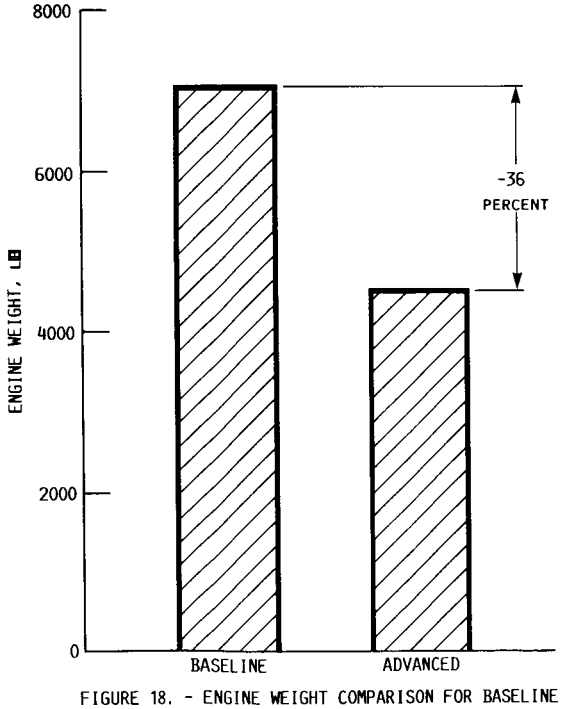

FIGURE 18. - ENGINE WEIGHT COMPARISON FOR BASELINE AND ADVANCED TURBOFAN.

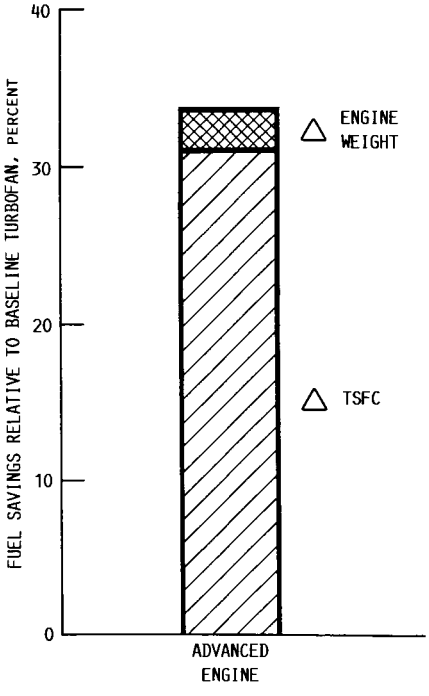

FIGURE 19. - ADVANCED ENGINE FUEL SAVING RELATIVE TO BASELINE TURBOFAN. MISSION: MACH 0.8; RANGE, 5500 N MI; PAYLOAD, 500 PASSENGERS.

APPENDIX A

SYMBOL LIST

AR	aspect ratio
BPR	bypass ratio
D_{HUB}	fan hub diameter, ft
D_{MAX}	fan maximum cowl diameter, ft
D_{TIT}	fan tip diameter, ft
FPR	fan pressure ratio; bypass/core
FN	engine net thrust, lb
g	gravitational constant, ft/sec^2
HPC	high pressure compressor
HPT	high pressure turbine
J	mechanical equivalent of heat, 778 ft-lb/BTU
K	corrected flow per unit area, lb/sec-ft^2
L/D	nacelle fineness ratio
LPC	low pressure compressor
LPT	low pressure turbine
N	number of stages
OPR	overall pressure ratio
P/P,PR	pressure ratio
P_T	total pressure, lb/in.^{2}
T_g	hot gas temperature, °R
T_m	bulk metal temperature, °R
T_3	HPC exit temperature, °R
T_{41}	turbine ratio-inlet temperature, °R
TSFC	thrust specific fuel consumption, lb/lb-hr
U_m	mean blade velocity, ft/sec
V_T	tip velocity, ft/sec
W_c	core airflow, lb/sec
ΔH	enthalpy change btu/lb
$\Delta P/P$	pressure loss
θ	temperature/sea-level standard temperature
γ	ratio of specific heats
η	efficiency
σ	D_{max}/D_{TIP}

Subscripts

ad	adiabatic
j	stage
ov	overall
p	polytropic

APPENDIX B

FLOWPATH STUDY

Very advanced lightweight composite materials such as discussed in the present study may lead to even higher stage pressure ratios, tip speeds and, hence, fewer and lighter weight compressor and/or turbine stages. To reduce the number of stages of compression, a number of factors must be considered. Two of these are blade loading and tip speed. Too high of a blade loading may result in flow separation losses; too high of a tip speed may result in shock losses. Thus, one may have to trade one off against the other to reduce the number of stages while at the same time achieving the aggressive advanced engine component efficiencies. Changes to the compressor and their affects on the turbine and the flowpath must also be considered in terms of engine TSFC and weight.

High Pressure Compressor (HPC)

For the present study, two methods or paths for achieving higher blade loadings and/or tip velocities were considered to determine possible tradeoffs, limitations (relative to the compressor and turbine flowpaths, stresses, etc.), and payoffs. These paths (denoted as A and B) are illustrated in figure 20. With path A both the compressor tip velocity and stage pressure ratio are increased in such a manner that the blade loading remains constant. For path B the tip velocity remains constant and the stage pressure ratio is increased, thereby, reducing the number of stages and increasing the blade loading for a given overall compressor pressure ratio. Based on a constant blade loading of 0.55 (path A) for the advanced HPC, figure 21 shows the variation in first stage pressure ratio as a function of corrected tip velocity. The increase in first stage pressure ratio allows a reduction in the number of HPC stages from 12 to 10 for an overall pressure ratio of 22.2. In contrast the HPC of the baseline engine has a first stage pressure ratio of 1.466, a corrected tip velocity of 1284 ft/sec (roughly 200 ft/sec lower), a loading of 0.69, and a pressure ratio of 14 (in 10 stages). The work factor ($gJ\ \Delta H/N/U_m^2$) and the number of stages (three HPT and five LPT) were specified for the advanced engine. As a result, for path A the HPT mean diameter decreased by 12 percent as the compressor corrected tip velocity increased from 1536 to 1712 ft/sec. The maximum blade pull stress for the HPC increased from 54 000 to 67 000 psi (24 percent) versus 43 000 psi for the baseline engine. Similarly the maximum pull stress for the HPT increased by 27 percent, due mainly to the required change in the hub-tip ratio to accommodate the airflow when designed with a fixed turbine loading parameter. The resulting changes in engine TSFC and weight are shown in figures 22 and 23. Reducing the number of HPC stages from 12 to 10 results in a slight increase in TSFC (fig. 22) as a result of a decrease in compressor efficiency. Engine weight decreased by about 1 percent (fig. 23).

For path B the blade loading for the HPC was increased from the previous value of 0.55 to 0.61 by reducing the number of stages from 11 to 10 while maintaining the same corrected tip speed (1617 ft/sec). As with the results for path A, the TSFC changed only slightly; while engine weight (fig. 24) for path B decreased by about 0.5 percent (about the same as for path A). The tip velocity for the 10-stage HPC of path B is about 100 ft/sec lower than that of path A. As a result, the compressor blade pull stress is slightly lower

(59 000 versus 67 000 psi). Based on the change in TSFC, engine weight, stress level, etc., the decision between paths A and B (or a compromise) may depend on tradeoffs required to attain the levels of efficiency used in the study and possible turbine limitations. As a result of this brief study and the cycle study, an 11-stage HPC was selected for the advanced engine. However, before deciding on a compressor tip velocity (and therefore blade loading), possible turbine limitations were considered. A similar study was performed for the LPC.

Low Pressure Compressor (LPC)

The previous figures were based on a three-stage LPC. Figures 25 and 26 show the effect on TSFC and engine weight of reducing the number of LPC stages from three to two with an 11-stage HPC. Compared with a three-stage LPC, two stages result in a slight increase in TSFC (fig. 25), due mainly to the decrease in the efficiency of the LPC. Engine weight, however, decreased by 4.4 percent largely due to the decrease in the weight of the low pressure spool (fig. 26). The decrease in the number of LPC stages results in a 12 percent decrease in the weight of the LPC. The weight of the LPT decreases by 13.7 percent due to the reduction in the diameter of the turbine. The diameter decreases to maintain about the same tip velocity (based on a constant LPT work factor). To accommodate the flow at the lower Mach number (for the two-stage LPC), the hub-tip ratio of the LPT decreased resulting in a blade pull stress of 98 000 psi (a 60 percent increase). The decrease in engine weight for the two-stage LPC is offset somewhat by the increased weight of the gearbox (12 percent). However, a pull stress of this magnitude for an advanced material may be unacceptable.

To reduce the blade pull stress levels associated with the HPC and the LPT of the two-stage LPC engine, compressor tip speeds and, therefore, shaft speed for both spools of the engine were reduced. As a result, the maximum blade pull stress for the HPC decreased from 60 000 to 44 000 psi as the corrected tip speed was reduced from 1617 to 1392 ft/sec. Similarly the blade pull stress for the LPT decreased from 98 000 to 78 000 psi by decreasing the corrected tip speed of the LPC from 1986 to 1723 ft/sec. With these decreases in tip velocity, the blade loading for the LPC and the HPC increased from 0.36 and 0.55 to 0.46 and 0.741, respectively. The effect of these changes on engine TSFC and weight is shown in figures 27 and 28. Again, TSFC is affected only slightly, while engine weight increased about 1 percent.

Turbines

The previous engines used a three-stage HPT. For the lowest HPC corrected tip velocity (1392) ft/sec of figure 28, the number of stages for the HPT was decreased to two. The effect on engine TSFC and weight is shown in figures 29 and 30. Engine TSFC is slightly higher for the two stage HPT due to the lower turbine efficiency. The decrease in turbine weight associated with the two-stage HPT is offset by the increased weight of the five-stage LPT. The weight of the LPT increases due to the decrease in the required hub-tip ratio and the resulting increase in blade pull stress. As a result engine weight increases by 0.5 percent when decreasing the number of HPT stages from three to two. However, the cost of a two-stage HPT may be lower (beyond the scope of the present study). The flow path for the advanced engine having a two stage HPT

is shown in figure 31. The engine has a maximum diameter of 106 in. and is 110 in. long up to the exit of the LPT and 152 in. overall to the exit of the nozzle. Engine weight includes all of the components shown in the figure plus the gearbox.

To reduce the displacement between the HPT and the LPT, the loading parameter for the HPT was decreased from 2.0 to 1.54. This increased the tip velocity from 1275 to 1460 ft/sec. As a result the exit tip radius increased by about 1 in. To further reduce the length of the transition duct, the loading parameter for the LPT was increased from 1.52 to 1.86 which results in only a 0.5 percent increase in TSFC (fig. 32), but an 11 percent decrease in engine weight (fig. 33).

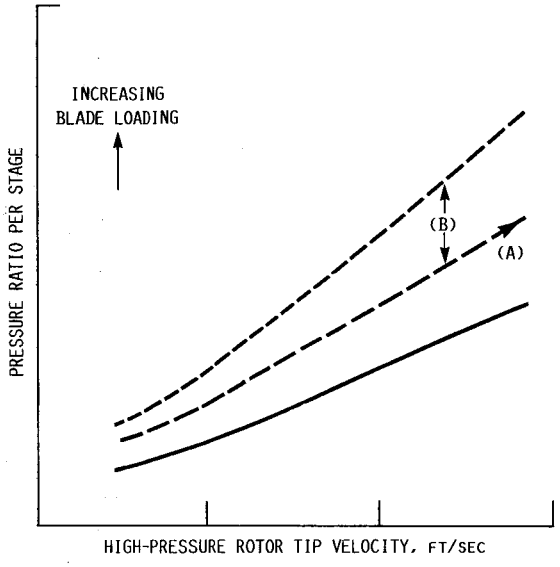

FIGURE 20. - COMPRESSOR STAGE PRESSURE RATIO TRENDS AS FUNCTION OF ROTOR TIP VELOCITY FOR RANGE OF BLADE LOADINGS.

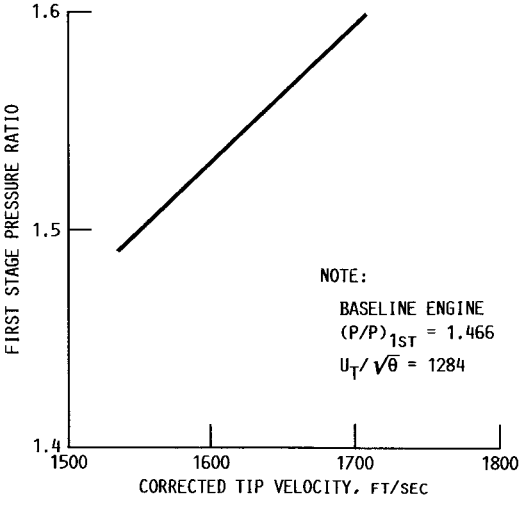

FIGURE 21. - ADVANCED AXIAL COMPRESSOR STAGE PRESSURE RATIO VERSUS CORRECTED TIP VELOCITY. FIRST STAGE BLADE LOADING IN HPC, 0.55; HPC PRESSURE RATIO, 22.2.

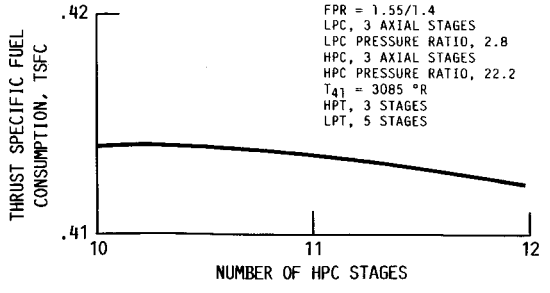

FIGURE 22. - ADVANCED ENGINE PERFORMANCE VERSUS NUMBER OF HIGH-PRESSURE COMPRESSOR STAGES. BLADE LOADING FOR LPC, 0.38; FOR HPC, 0.55.

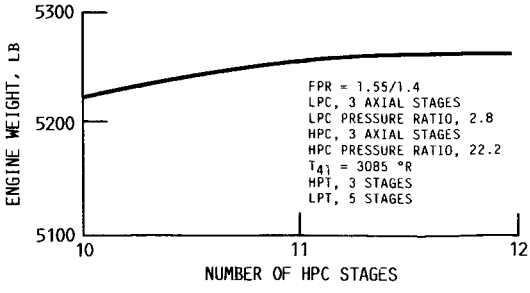

FIGURE 23. - ADVANCED ENGINE WEIGHT VERSUS NUMBER OF HIGH-PRESSURE COMPRESSOR STAGES. BLADE LOADING FOR LPC, 0.38; FOR HPC, 0.55.

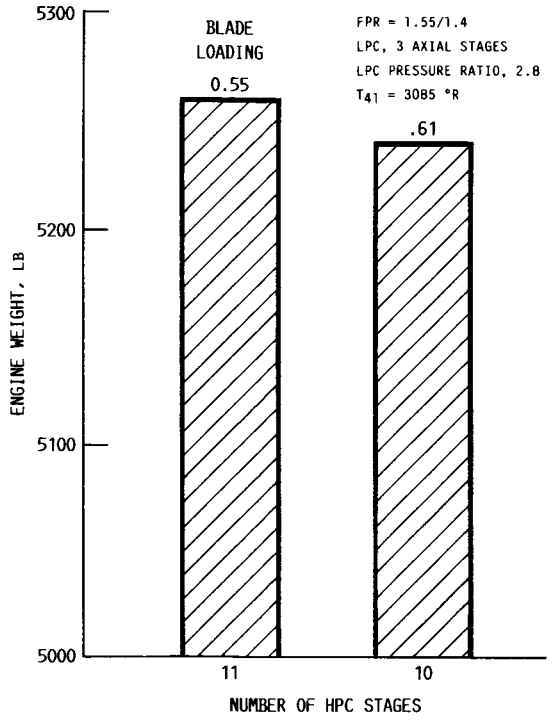

FIGURE 24. - ADVANCED ENGINE WEIGHT VERSUS NUMBER OF HIGH-PRESSURE COMPRESSOR STAGES FOR CONSTANT CORRECTED TIP VELOCITY.

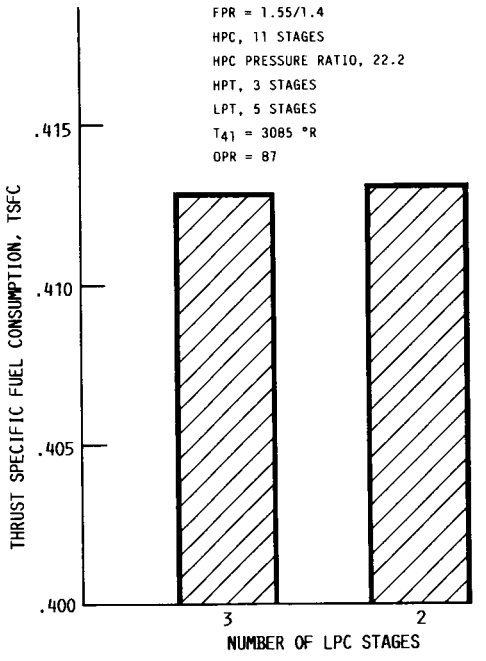

FIGURE 25. - EFFECT ON ENGINE TSFC OF REDUCING THE NUMBER OF LOW-PRESSURE COMPRESSOR STAGES OF ADVANCED ENGINE.

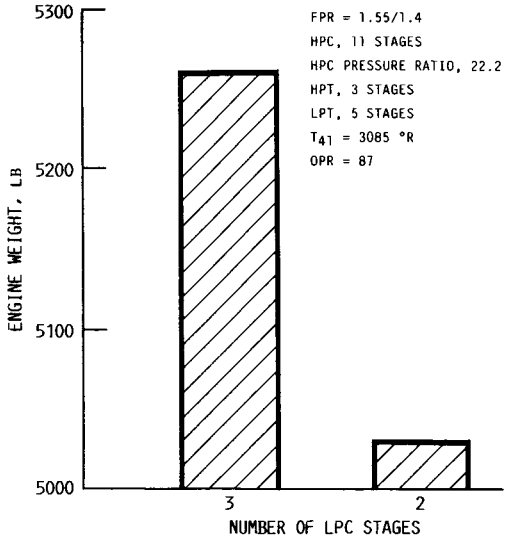

FIGURE 26. - EFFECT ON ENGINE WEIGHT OF REDUCING THE NUMBER OF LOW-PRESSURE STAGES OF THE ADVANCED ENGINE.

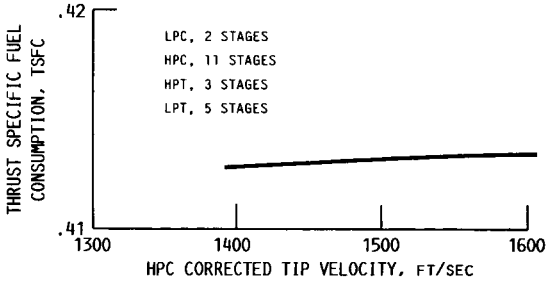

FIGURE 27. - ADVANCED ENGINE PERFORMANCE AS FUNCTION OF CORRECTED TIP VELOCITY FOR HIGH-PRESSURE COMPRESSOR, CONSTANT STAGE PRESSURE RATIO.

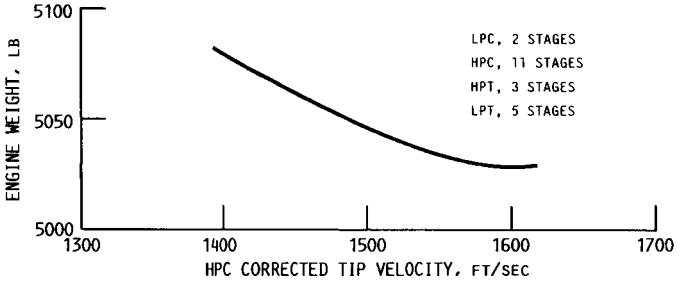

FIGURE 28. - ADVANCED ENGINE WEIGHT AS FUNCTION OF CORRECTED TIP VELOCITY FOR THE HIGH-PRESSURE COMPRESSOR WITH CONSTANT STAGE PRESSURE RATIO.

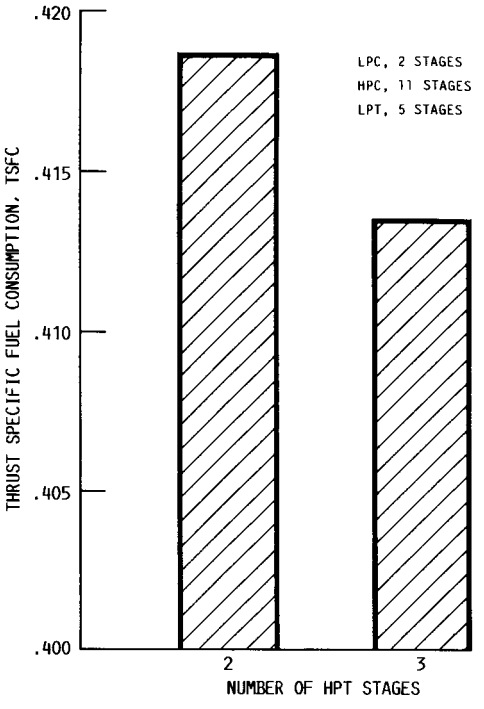

FIGURE 29. - EFFECT ON TSFC OF DECREASING NUMBER OF HIGH-PRESSURE TURBINE STAGES OF ADVANCED ENGINE.

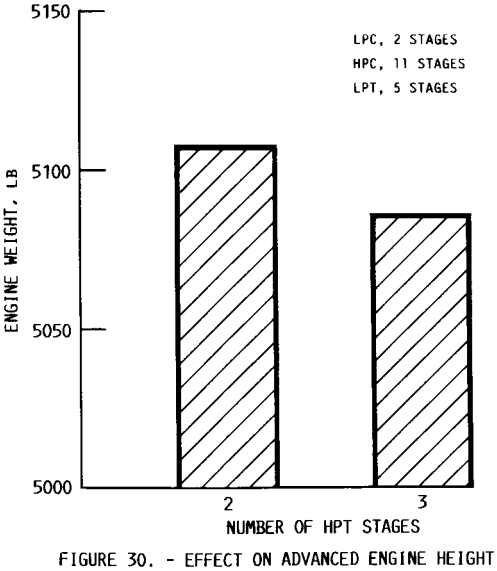

FIGURE 30. - EFFECT ON ADVANCED ENGINE HEIGHT OF DECREASING THE NUMBER OF HIGH-PRESSURE TURBINE STAGES.

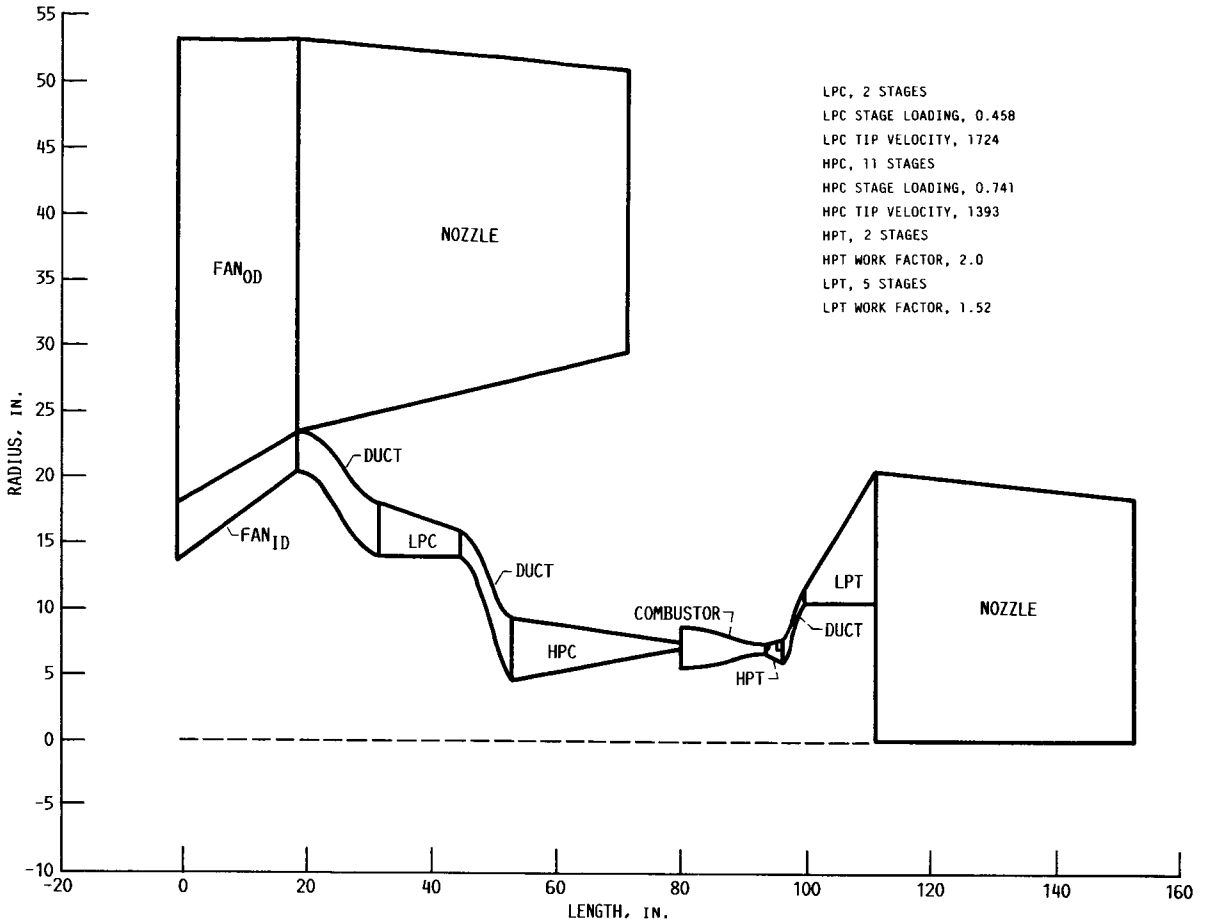

FIGURE 31. - ADVANCED ENGINE FLOW PATH. TOTAL ENGINE WEIGHT, 5107 LB.

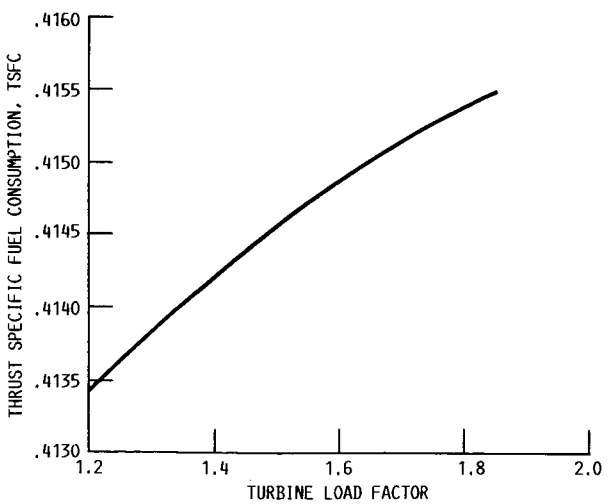

FIGURE 32. - ADVANCED ENGINE PERFORMANCE AS FUNCTON OF LOW-PRESSURE TURBINE LOADING FACTOR.

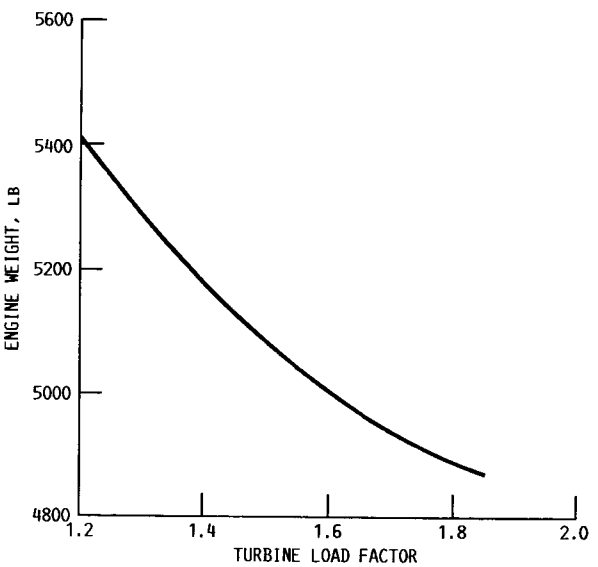

FIGURE 33. - ADVANCED ENGINE WEIGHT AS FUNCTION OF LOW-PRESSURE TURBINE LOADING FACTOR.

1. Report No.	2. Government Accession No.	3. Recipient's Catalog No.
NASA TM-89868		

4. Title and Subtitle	5. Report Date
Analysis of an Advanced Technology Subsonic Turbofan Incorporating Revolutionary Materials	May 1987
	6. Performing Organization Code: 505-69-41

7. Author(s)	8. Performing Organization Report No.
Gerald Knip, Jr.	E-3542
	10. Work Unit No.

9. Performing Organization Name and Address	11. Contract or Grant No.
National Aeronautics and Space Administration Lewis Research Center Cleveland, Ohio 44135	
	13. Type of Report and Period Covered: Technical Memorandum

12. Sponsoring Agency Name and Address	14. Sponsoring Agency Code
National Aeronautics and Space Administration Washington, D.C. 20546	

15. Supplementary Notes

16. Abstract

Future implementation of revolutionary composite materials in an advanced turbofan offers the possibility of improved engine performance and reduced weight. This study determines the approximate optimum engine cycle, configuration, performance, and fuel saving for an early 21st century subsonic all-composite materials transport engine relative to a current technology baseline engine. The resultant advanced, uncooled engine has an overall pressure ratio of 87, a bypass ratio of 18, and a turbine rotor-inlet temperature of 3085 °R. Relative to the baseline engine, the advanced engine yields a 22 percent improvement in cruise TSFC and a 36 percent reduction in engine weight. Together these improvements result in a 33 percent fuel savings for an intercontinental quadjet having a design range of 5500 nmi and a payload of 500 passengers.

17. Key Words (Suggested by Author(s))	18. Distribution Statement
A/C propulsion Turbofan Composite materials	Unclassified - unlimited STAR Category 07

19. Security Classif. (of this report)	20. Security Classif. (of this page)	21. No. of pages	22. Price*
Unclassified	Unclassified	23	A02

*For sale by the National Technical Information Service, Springfield, Virginia 22161